THE JOURNAL OF BIOLOGICAL CHEMISTRY VOL. 284, NO. 22, pp. 14819–14827, May 29, 2009

Topogenesis of Mammalian Oxa1, a Component of the Mitochondrial Inner Membrane Protein Export Machinery*[S]

Received for publication, December 18, 2008, and in revised form, January 21, 2009 Published, JBC Papers in Press, April 6, 2009, DOI 10.1074/jbc.M809520200

Takashi Sato[1] **and Katsuyoshi Mihara**[2]

From the Department of Molecular Biology, Graduate School of Medical Sciences, Kyushu University, Fukuoka 812, Japan

Oxa1 is a mitochondrial inner membrane protein with a predicted five-transmembrane segment (TM1~5) topology in which the N terminus and a hydrophilic loop, L2, are exposed to the intermembrane space and the C-terminal region and two loops, L1 and L3, are exposed to the matrix. Oxa1 mediates the insertion of mitochondrial DNA-encoded subunits of respiratory complexes and several nuclear DNA-encoded proteins into the inner membrane from the matrix. Compared with yeast Oxa1, little is known about the import and function of mammalian Oxa1. Here, we investigated the topogenesis of Oxa1 in HeLa cells using systematic deletion or mutation constructs and found that (i) the N-terminal 64-residue segment formed a presequence, and its deletion directed the mature protein to the endoplasmic reticulum, indicating that the presequence arrests cotranslational activation of the potential endoplasmic reticulum-targeting signal within mature Oxa1, (ii) systematic deletion of Oxa1 TM segments revealed that the presence of all five TMs is essential for efficient membrane integration, (iii) the species-conserved hexapeptide (GLPWWG) located near the N terminus of TM1 was essential for export of the N-terminal segment and L2 into the intermembrane space from the matrix, *i.e.* for correct topogenesis of Oxa1, and (iv) GLPWWG placed near the N terminus of TM2 or TM3 in the reporter construct also supported its membrane integration in the Nout-Cin orientation. Together, these results demonstrated that topogenesis of Oxa1 is a cooperative event of all five TMs, and GLPWWG followed immediately by TM1 is essential for correct Oxa1 topogenesis.

Most mitochondrial proteins are nuclear DNA-coded, and their import into mitochondrial compartments, that is, the mitochondrial outer membrane (MOM),[3] mitochondrial inner membrane (MIM), intermembrane space (IMS), and matrix, is mediated by five protein translocation systems: translocase of the outer membrane (TOM complex), sorting and assembly machinery of MOM (SAM/TOB), translocases of the inner membrane (TIM23 complex and TIM22 complex), and a fifth system in the MIM that mediates integration of proteins from the matrix into the MIM (1, 2). The last system, which has been analyzed in detail in yeast, requires a membrane potential across the MIM and matrix ATP and mediates MIM integration of the mtDNA-encoded proteins as well as the integration of certain nuclear DNA-encoded proteins considered to be of bacterial origin, such as cytochrome *c* oxidase subunit II, F1Fo-ATPase subunit 9, and Oxa1 (3–5). Translocation efficiency is affected by the charge difference across the transmembrane (TM) in accordance with the positive-inside rule (5). Furthermore, the matrix-exposed C-terminal segment of Oxa1 is essential for binding mitochondrial ribosomes during cotranslational integration of mtDNA-encoded proteins (6, 7). Recent reports further demonstrated that the MIM protein Mba1, as a ribosome receptor, cooperates with the C-terminal ribosome binding segment of Oxa1 (8). The machinery and the underlying mechanisms of MIM insertion from the matrix must be further analyzed.

Oxa1 protein, originally identified in yeast, is a component of the matrix-to-MIM export system conserved from prokaryote to eukaryote and is involved in Oxa1 biogenesis (9–14). YidC, a bacterial homologue of Oxa1, is involved in the biogenesis of inner membrane proteins in a Sec-dependent or Sec-independent manner (15, 16). In yeast, IMS export from the matrix of the Oxa1 N-terminal segment emerging from the Tim23 channel requires a membrane potential (4, 17), and the export is compromised in mitochondria isolated from a temperature-sensitive Oxa1-expressing strain at a non-permissive temperature (12). Herrmann and Bonnefoy (18) reported that Oxa1 protein functions in the export of a single hydrophilic loop region that was artificially produced by ligating the C-terminal region of cytochrome *b* with cytochrome *c* oxidase subunit II and placed between TM segments. Direct interaction of Oxa1 with an immature subunit in complex V was observed during its biogenesis (19). So far, these studies have only been performed in yeast, and no information is available on the mechanism of topogenesis in mammals with regard to how Oxa1 is involved in the export of multiple regions in a protein molecule. Our *in vivo* study revealed that the correct topogenesis of Oxa1 in the MIM proceeds as a result of the cooperation of all five TMs and that the cooperation of TM1 and the species-conserved six-residue segment (GLPWWG) in the N-terminal flanking region is essential for export from the matrix of both the N-terminal segment and hydrophilic L2 into the IMS.

* This work was supported by grants from the Ministry of Education, Science, and Culture of Japan, Human Frontier Science Program, Core Research from Evolutional Science and Technology, and Takeda Science Foundation.

[S] The on-line version of this article (available at http://www.jbc.org) contains supplemental Figs. 1–4.

[1] Present address: Dept. of Pathophysiological Science, Faculty of Pharmaceutical Sciences, Hokuriku University, Ho-3 Kanagawa-machi, Kanazawa 920-1181, Japan.

[2] To whom correspondence should be addressed. Tel.: 81-92-642-4709; Fax: 81-92-642-6768; E-mail: mihara@cell.med.kyushu-u.ac.jp.

[3] The abbreviations used are: MOM, mitochondrial outer membrane; MIM, mitochondrial inner membrane; IMS, intermembrane space; ER, endoplasmic reticulum; TM, transmembrane; rOxa1, rat Oxa1 protein; siRNA, short inhibitory RNA; MTS, matrix targeting signal; HA, hemagglutinin.

EXPERIMENTAL PROCEDURES

Materials—The following antibodies were obtained from the indicated sources: rabbit polyclonal antibodies against hemagglutinin (HA) tag (Covance, Berkeley, CA), mouse anti-T7 monoclonal antibody (Novagen, Darmstadt, Germany), and mouse monoclonal antibody against human Oxa1 (BD Biosciences). Rabbit anti-Tim23 and anti-Tim44 polyclonal antibodies were obtained as described previously (20). Other chemicals were purchased from Wako Pure Chemicals (Osaka, Japan).

Isolation of Rat Oxa1 Protein (rOxa1) cDNA—A cDNA of rOxa1 was isolated from a rat liver cDNA library using a reverse transcriptase based-method (SuperScript, Invitrogen). Oligonucleotides were designed according to a rat-expressed sequence tag data base. PCR products amplified with 5′-AAGCTTGCCACCATGGGTTCAGTTTGCCGTCGC-3′ and 5′-TCTAGAGCCGAGTGTGTCCTGCCACGGCTT-3′ were digested with HindIII/XbaI. The fragments were ligated into a HindIII/XbaI-digested mammalian expression vector, pRcCMV (Invitrogen). The amino acid homology of rOxa1 to other species was 35% (yeast), 65% (human), and 87% (mouse; supplemental Fig. 1).

Modification of rOxa1 for Analyses of Mitochondrial Targeting Signal and N-terminal Export—All constructs with an HA tag at the C-terminal portion were generated using PCR and expressed in HeLa cells. To analyze the rOxa1 targeting signal, we constructed the following deletion proteins: rOxa1Δ(1–44) lacking amino acid residues 1–44, rOxa1Δ(1–64) lacking amino acid residues 1–64, rOxa1Δ(18–44) lacking amino acid residues 18–44, and rOxa1Δ(1–29) lacking amino acid residues 1–29. The T7 tag was introduced to the 70th amino acid from the N terminus of rOxa1 (70T7) to examine the N-terminal export to the IMS. The T7 tag was also inserted at amino acid residue 238 (238T7) to study translocation of the loop between TM2 and TM3 into the IMS.

Construction of rOxa1-dihydrofolate Reductase or Green Fluorescent Protein Fusion Proteins—The following portions of rOxa1 were used to generate the fusion proteins (designated in parentheses): N-terminal residues 44 (N44), 100 (N100), 135 (N135), 144 (N144), 147 (N147), and 153 (N153) and transmembrane segment 1 (TM1), 1 and 2 (TM(1–2)), 1, 2, and 3 (TM(1–3)), 1, 2, 3, and 4 (TM(1–4)), and 1, 2, 3, 4, and 5 (TM(1–5)). TM1 of the fusion construct was replaced with TM2 or TM3 to create fusion proteins TM2 and TM3, respectively. Each segment was amplified by PCR and fused with the folding incompetent (methotrexate-insensitive) dihydrofolate reductase-HA (21) or green fluorescent protein.

Glycine Scanning—Amino acid residues in the conserved "GLPWWG" region located in the N-terminal flanking region of TM1 were substituted with glycine using PCR to obtain D128G, L129G, L131G, P132G, W133G, W134G, A136G, and W133G/W134G.

Analysis of Intracellular Localization of rOxa1 Using Fluorescence Microscopy—Immunofluorescence microscopy was performed to examine intracellular localization of rOxa1. Anti-calnexin antibody (Stressgen Biotechnologies, British Columbia, Canada) was used to identify the ER. Mitochondria were visualized with MitoTracker Red (Invitrogen). rOxa1-HA, rOxa1Δ(1–44), and rOxa1Δ(1–64) were detected by anti-HA antibody followed by a secondary fluorescein-labeled or Texas Red-labeled secondary antibody.

Cell Fractionation and Protease Protection Experiments—After a 24-h incubation after transfection with FuGENE 6 (Roche Diagnostics), HeLa cell suspensions were homogenized by passing back and forth 15 times through a 27-gauge needle attached to a 1-ml syringe in homogenization buffer (10 mM Hepes-KOH buffer (pH 7.4) containing 1 mM EDTA, 0.25 M sucrose, and protease inhibitor mixture, Complete (Roche Diagnostics)). Mitochondria were isolated by differential centrifugation. For protease protection experiments, mitochondria (40 μg) were incubated in the presence or absence of digitonin (final concentrations, 0.08, 0.1, or 0.12%) or 1% Triton X-100 on ice for 10 min followed by the treatment of 0.1 mg/ml proteinase K on ice for 30 min. The reaction was stopped by adding trichloroacetic acid. In the alkaline treatment experiment, mitochondria were incubated in 0.1 M Na_2CO_3 on ice for 30 min followed by ultracentrifugation to separate the supernatant and membrane fractions, which were subjected to SDS-PAGE and subsequent immunoblotting. The filters were incubated with horseradish peroxidase-labeled secondary antibodies, and bands were detected with ECL reagent (Amersham Biosciences).

Knockdown of Human Oxa1 in HeLa Cells—A double-stranded short inhibitory RNA (siRNA) targeting human Oxa1 protein (5′-CAACGCAUGCGGAAUCAGU-3′) was transfected into HeLa cells using Lipofectamine 2000 (Invitrogen). The protein expression was monitored 24 or 48 h after the transfection. For evaluation of the N-terminal export in the Oxa1 knockdown cells, N153 or 238T7 was transfected with FuGENE 6 24 h after siRNA (100 nM) introduction. The N-terminal export and the translocation of loop region L2 were examined 15 h after transfection.

RESULTS

Submitochondrial Localization of rOxa1—Immunofluorescence microscopy showed that C-terminal HA-tagged rOxa1 (rOxa1-HA) expressed in HeLa cells colocalized with MitoTracker Red (supplemental Fig. 2). Comparison of SDS-PAGE mobility of *in vivo* and *in vitro* expressed forms revealed that rOxa1-HA is synthesized as a preprotein with a size ~6.8 kDa higher than that of the mature form (Fig. 1*B*). The construct in which the N-terminal 64-residue segment of rOxa1-HA was deleted, rOxa1Δ(1–64), had the same mobility as HeLa cell-expressed rOxa1-HA on SDS-PAGE, suggesting that the processing point was likely located between amino acid residues 64 and 65 (Fig. 1*C*, *lanes 1* and *2*).

The matrix-targeting signal-truncated versions rOxa1-HA, rOxa1Δ(1–44), and rOxa1Δ(1–64) failed in mitochondrial localization and showed an ER distribution, indicating that TMs present in the mature domain act as ER-targeting and insertion signals (supplemental Fig. 2) whose function was suppressed by the N-terminal presequence, as is the case for ABCme, a half ABC transporter of MIM (22). To examine submitochondrial localization, the mitochondria were isolated from HeLa cells and treated with proteinase K in low concen-

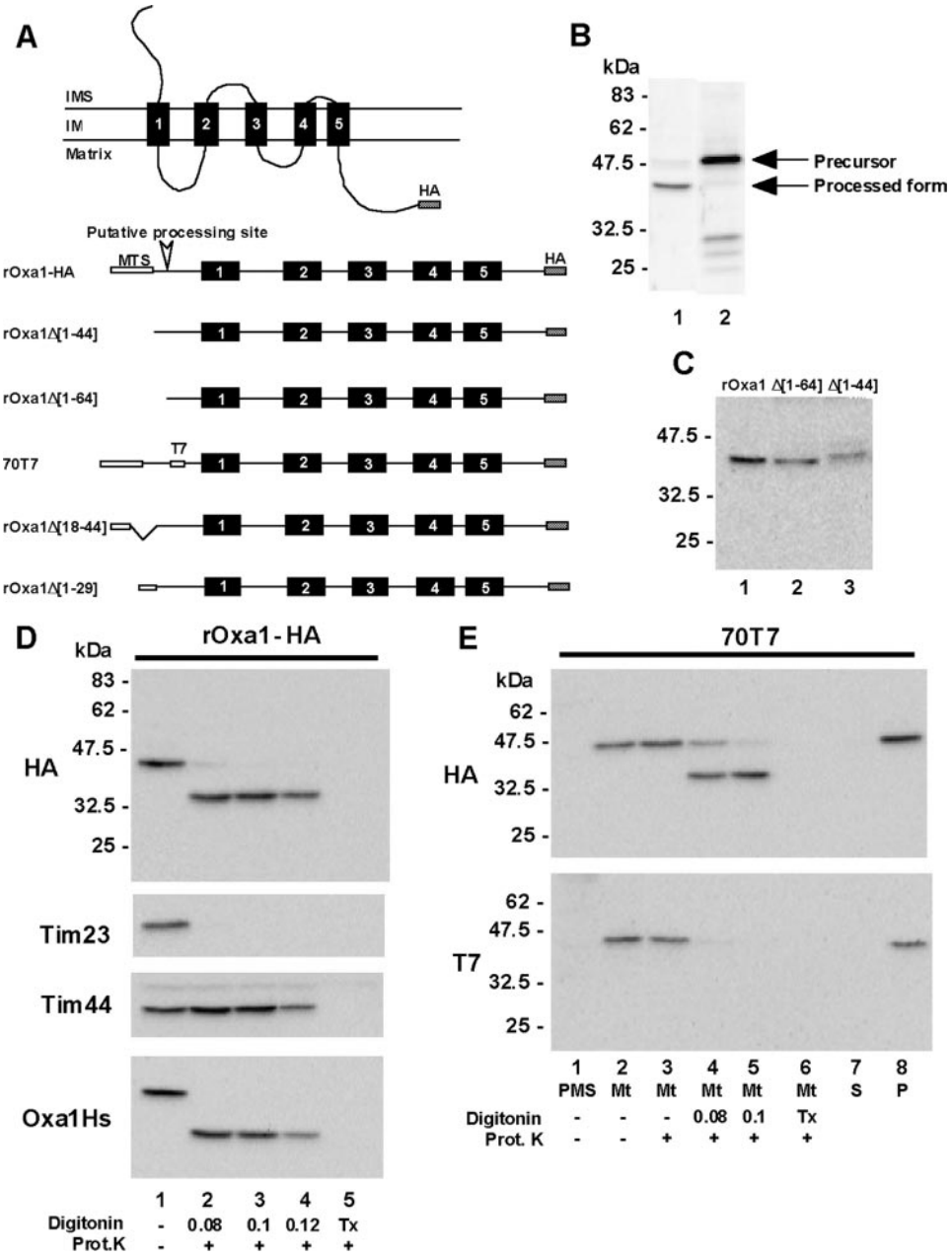

FIGURE 1. **Mitochondria-targeting signal of rOxa1.** *A*, schematic diagram of rOxa1. rOxa1Δ(1–44) and rOxa1Δ(1–64) lack amino acid residues 1–44 and 1–64, respectively; 70T7 has a T7 tag inserted between amino acid residues 69 and 70; rOxa1Δ(18–44) and rOxa1Δ(1–29) lack amino acid residues 18–44 and 1–29, respectively. All constructs have HA tags. *B*, comparison of mobility in the electrophoresis between rOxa1-HA expressed in HeLa cells (*lane 1*) and its *in vitro* translation product using rabbit reticulocyte lysate (*lane 2*). rOxa1 was analyzed with Western blotting using anti-HA antibody. *C*, estimation of the processing site of rOxa1 expressed in HeLa cells by electrophoresis mobility analysis. rOxa1-HA (*lane 1*; mitochondrial fraction), rOxa1Δ(1–64) (*lane 2*; post-mitochondrial supernatant), and rOxa1Δ(1–44) (*lane 3*; post-mitochondrial supernatant) were expressed in HeLa cells followed by Western blotting. *D*, effect of digitonin concentration on the permeability of mitochondrial outer and inner membranes. Mitochondria from HeLa cells expressing rOxa1-HA were treated with proteinase K (*Prot. K*) (0.1 mg/ml) in the presence of the indicated concentrations of digitonin or 1% Triton X-100 (*Tx*). The resulting samples were analyzed by SDS-PAGE and subsequent Western blotting. *E*, protease protection analysis of mitochondria from HeLa cells expressing 70T7. Submitochondrial localization was examined after the protease treatments, as described in *D*. In a different experiment the mitochondria (*Mt*) were treated by 0.1 M Na_2CO_3, centrifuged to separate the supernatant (*S*) and membrane (*P*) fractions, and subsequently analyzed by SDS-PAGE and Western blotting. PMS, postmitochondrial supernatant.

trations of digitonin. The 41-kDa rOxa1-HA band was shifted to 33 kDa in the presence of 0.08–0.10% digitonin (Fig. 1*D*, *lanes 1–3*). Under this condition, Tim23, which is embedded in the MIM through four hydrophobic TMs, extruding a bulk N-terminal segment to the IMS, was degraded by the protease (Fig. 1*D*, *lanes 2* and *3*), indicating that the MOM was permeabilized. A matrix marker, Tim44, on the other hand, was protected from protease treatment under these conditions, indicating that the MOM was specifically permeabilized by 0.08- 0.1% digitonin, whereas the MIM remained intact (Fig. 1*D*, *lanes 2* and *3*). The 33-kDa band was completely digested by proteinase K under 1% Triton X-100 (*lane 5*). These results indicated that mature rOxa1-HA was embedded in the MIM extruding the N-terminal segment to the IMS. The endogenously expressed human Oxa1 (Oxa1Hs) produced a similar protease protection pattern (Fig. 1*D*). Because mitochondria-imported rOxa1-HA was resistant to alkaline extraction, it was firmly inserted into the MIM (supplemental Fig. 3*A*, *lanes 7* and *8*). To analyze membrane orientation of the N-terminal segment of mature Oxa1, a T7 tag was introduced in the N terminus near TM1 of rOxa1-HA (70T7; Fig. 1*A*). Proteinase K treatment of mitochondria harboring 70T7 produced an HA-positive, but T7-negative, 33-kDa band under low digitonin concentrations (Fig. 1*E*, *lanes 3–5*). Together, these findings indicate that the N-terminal portion (71 residues) of mammalian Oxa1 was exposed to the mitochondrial IMS, whereas the C-terminal segment localized in the matrix. Hereafter, the proteinase K-resistant band produced by proteinase K after permeabilization of the MOM was monitored as a measure of MIM integration of Oxa1 constructs in the correct orientation.

Mitochondrial Targeting Signal of rOxa1—Fluorescence microscopy of fusion proteins comprising various lengths of the N-terminal portion of rOxa1 and green fluorescent protein revealed that the N-terminal 45 amino acids functioned as a mitochondrial targeting signal in rOxa1 (data not shown). To analyze the signal in more detail, the N-terminal 45-amino acid residue segment was partially deleted to generate rOxa1Δ(18–44) and rOxa1Δ(1–29) (supplemental Fig. 3). Both constructs

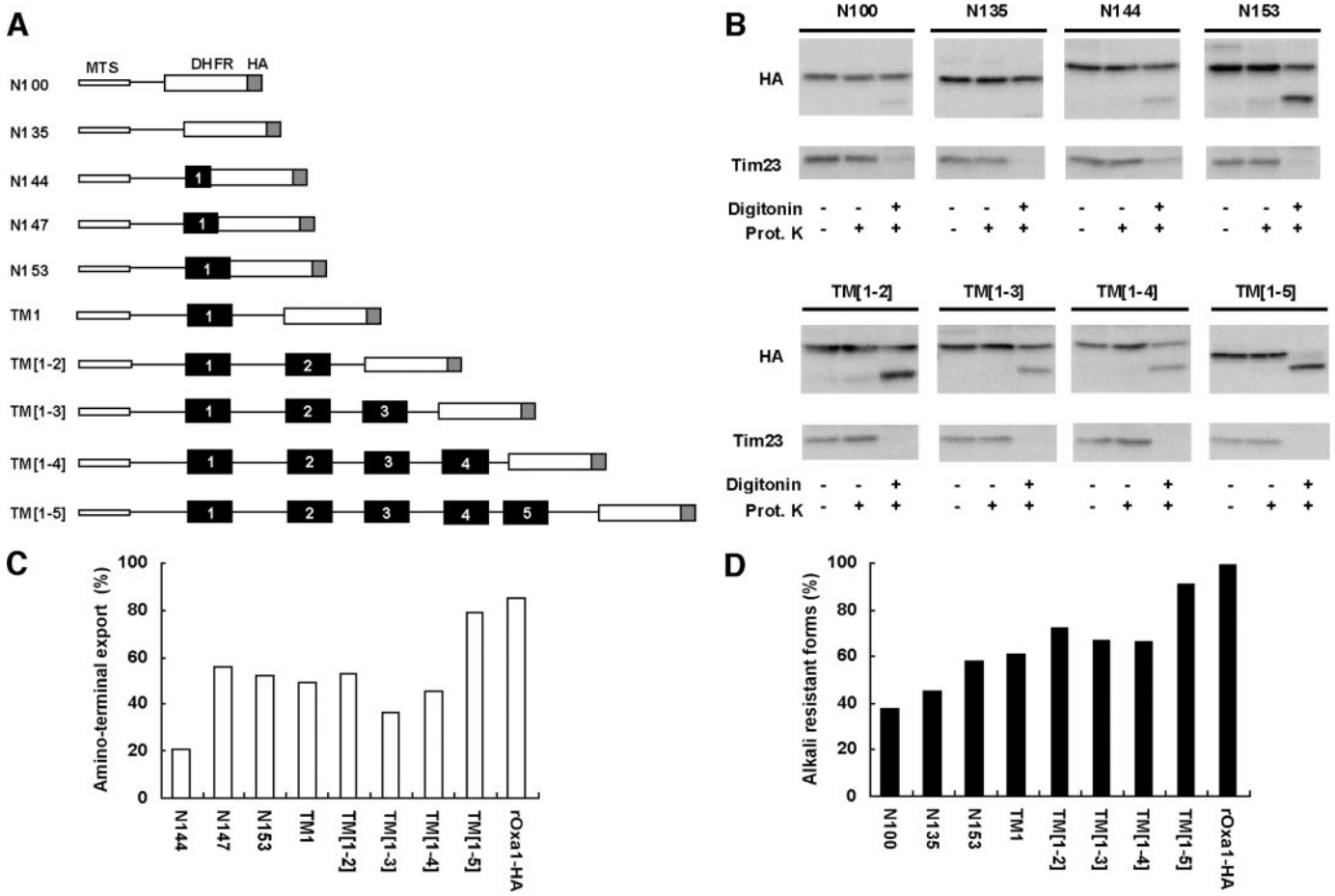

FIGURE 2. **Examination of submitochondrial localization of rOxa1-dihydrofolate reductase fusion proteins.** *A*, schematic diagram of the fusion proteins. *DHFR*, dihydrofolate reductase. *B*, protease protection analysis of the fusion proteins. Mitochondria were treated with proteinase K (*Prot. K*) in the presence of digitonin (0.1%) followed by SDS-PAGE and Western blotting using anti-HA antibody. *C*, densitometric analyses of the N-terminal export in the fusion proteins. Export efficiencies are expressed as a percentage of the proteinase K-shifted band of the total bands (sum of shifted and unshifted bands). *D*, densitometric analyses of alkaline-resistant fraction in the mitochondria imported total proteins.

expressed in HeLa cells were imported into mitochondria with lower efficiency compared with intact rOxa1, and a significant amount of the unprocessed form was detected in the post-mitochondrial supernatant and mitochondrial fractions, although rOxa1Δ(18–44) underwent efficient matrix targeting signal (MTS) processing by mitochondrial processing peptidase compared with rOxa1Δ(1–29) (supplemental Fig. 3*A*). Both constructs produced a mature protein band of 41 kDa, as did wild-type rOxa1-HA, indicating that the processing occurred at the same site as in the Oxa1 precursor, irrespective of the length of the MTS. The precursors of both constructs were sensitive to the externally added proteinase K (supplemental Fig. 3*A*, *lanes 10*, *11*, *18*, and *19*), and a significant fraction was resistant to alkali extraction (*lanes 15*, *16*, *23*, and *24*), indicating that translocation of both constructs was partially halted, thereby exposing the bulk portion to the cytoplasmic side. Moreover, rOxa1Δ(1–29) exhibited lower export efficiency of the N-terminal segment of the mature protein compared with rOxa1Δ(18–44) (supplemental Fig. 3*B*). Of note, rOxa1Δ(1–44) recovered in the mitochondrial fraction was completely degraded by externally added proteinase K (supplemental Fig. 3*A*, *lanes 26* and *27*). These findings indicated that the mitochondrial-targeting signal of rOxa1 was within the N-terminal 45-residue region that was composed of two potentially active segments, both of which were necessary for efficient import into the mitochondria. Notably, these results also indicate that the processing efficiency of the signal limits the export of the N-terminal portion of mature Oxa1.

All Five TMs Are Required for Efficient Integration of rOxa1 into the MIM—To analyze the regions responsible for rOxa1 topogenesis, various lengths of the N-terminal rOxa1 regions were fused to a reporter protein dihydrofolate reductase-HA, expressed in HeLa cells, and their intra-mitochondrial localization was analyzed by proteinase K digestion (Fig. 2*A*). These experiments revealed that the MTS in N100, N135, and N144 was efficiently processed and the mature proteins were translocated into the matrix (Fig. 2*B*). In the case of proteins containing the regions downstream from TM1 to TM4, approximately half of the fraction of each construct successfully integrated into the MIM in the correct topology, exposing the N-terminal region into the IMS and the C-terminal region in the matrix, whereas the other fraction was completely translocated from the MIM into the matrix (Fig. 2, *B* and *C*). In striking contrast, efficient N-terminal export and membrane integration were observed for the fusion protein containing all five TMs (Fig. 2, *B–D*). Furthermore, the extent of membrane

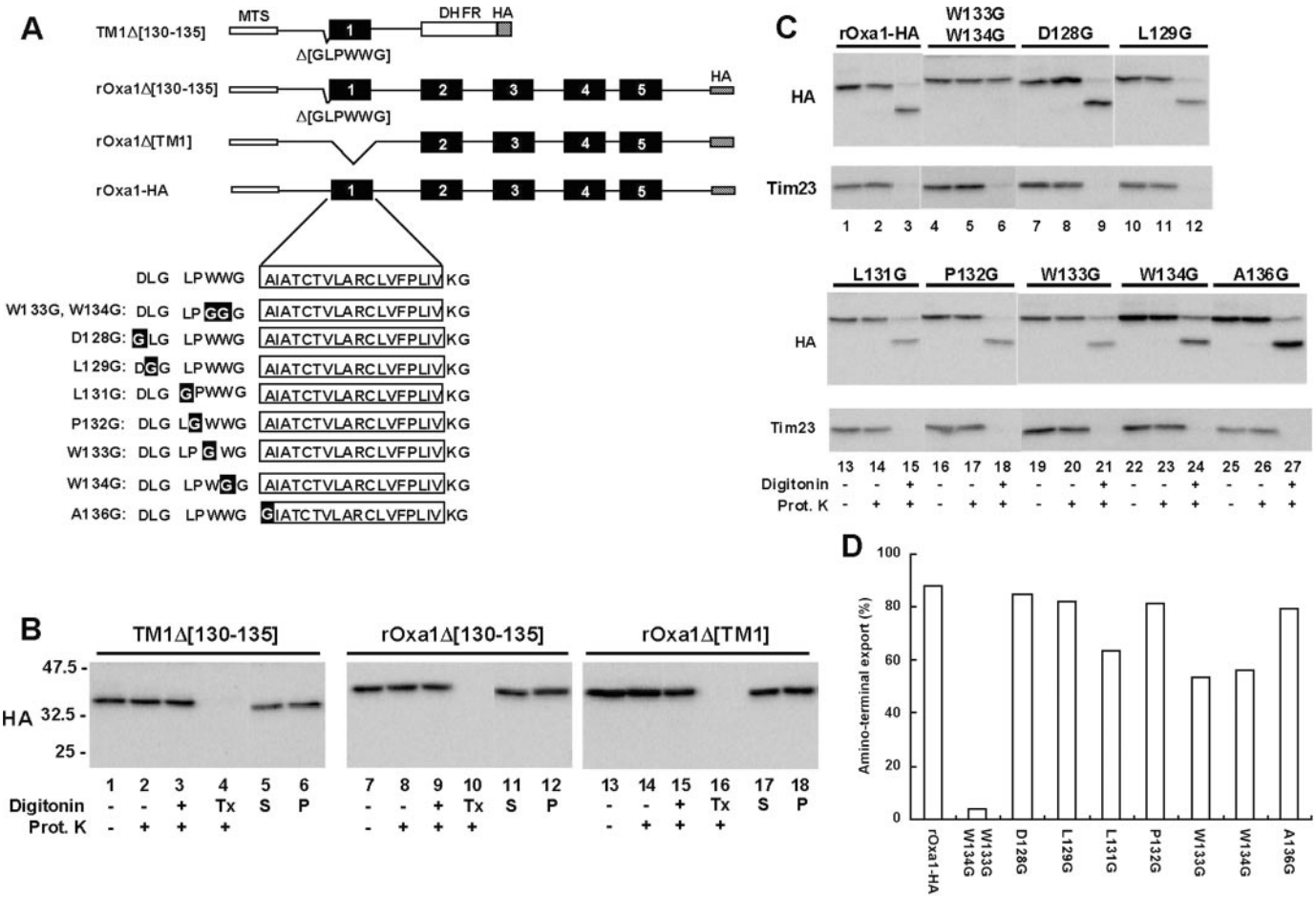

FIGURE 3. **Glycine-scanning experiments in the conserved GLPWWG region.** *A*, schematic diagram of the constructs with a deletion or with glycine substitution(s) in the conserved GLPWWG region of rOxa1. *DHFR*, dihydrofolate reductase. *B*, protease protection analysis of submitochondrial localization of TM1Δ(130–135), rOxa1Δ(130–135), and rOxa1Δ(TM1) expressed in HeLa cells. The mitochondria were treated with the protease in the presence of 0.1% digitonin or 1% Triton X-100 (*Tx*) as described in Fig. 1*E*. *Prot. K*, proteinase K. *C*, the N-terminal export of glycine-substituted mutants was examined after protease treatment in the presence of digitonin (0.1%), as described in Fig. 2*B*. *S*, supernatant; *P*, membrane fraction. *D*, densitometric analyses of the N-terminal export in the glycine-scanning experiments. N-terminal export (%) = exported form/sum of exported and unexported forms.

integration as assessed by alkali extraction was significantly lower for the constructs carrying incomplete sets of TMs compared with the constructs with a full set of the TMs (Fig. 2*D*). Taken together, these results indicated that all five TMs were required for the complete translocation of the N terminus into the IMS and the membrane integration of the remainder of the segment.

A Hexapeptide Sequence Near the N Terminus of TM1 Is Important for the N-terminal Export of rOxa1—The hexapeptide GLPWWG localized near the N terminus of TM1 is highly conserved in various species (supplemental Fig. 1). We, therefore, examined the involvement of this region for the N-terminal export. Constructs with deletions of this region, TM1Δ(130–135) and rOxa1Δ(130–135) (Fig. 3*A*), were efficiently imported into the matrix but failed to export the N-terminal segment into the IMS (Fig. 3*B*, *lanes 2*, *3*, *8*, and *9*); thus, transported constructs seemed to be weakly associated to the inner membrane because they were partially susceptible to alkali extraction (*lanes 5*, *6*, *11*, and *12*). The TM1-deleted rOxa1 also had severe export deficiency that was similar to the hexapeptide-deleted constructs (Fig. 3*B*, *lanes 2*, *3*, *8*, *9*, *14*, and *15*), whereas deletion of the other TMs resulted in milder inhibition of the export (Fig. 2, *B–D*). Together, these results clearly indicated that the hexapeptide and the region near TM1 are both essential for the IMS export of the N-terminal region and correct membrane integration of rOxa1. Considering that in rOxa1Δ(TM1) the hexapeptide is localized away from TM2, the hexapeptide seems to function only when located in the vicinity of TMs (see below).

Glycine scanning was performed to determine the amino acid residues in the hexapeptide that are responsible for N-terminal export (Fig. 3*A*). Glycine substitution at Leu-131, Trp-133, and Trp-134 impaired the N-terminal export activity (Fig. 3*C*, *lanes 13–15* and *19–24*, and D), and substitution of both Trp-133—Trp-134 with glycine (W133G, W134G) drastically inhibited N-terminal export (Fig. 3, *C*, *lanes 4–6*, and D). The W133G-W134G construct was also extracted with alkaline to the same extent as observed in the hexapeptide-deleted constructs TM1Δ(130–135) and rOxa1Δ(130–135) (data not shown). Glycine substitution of the amino acid residue in TM1 did not affect the N-terminal export activity (Fig. 3*C*, *lanes 25–27*, and *D*). These results indicated that L*X*WW in the hexapeptide sequence is critical for the export activity.

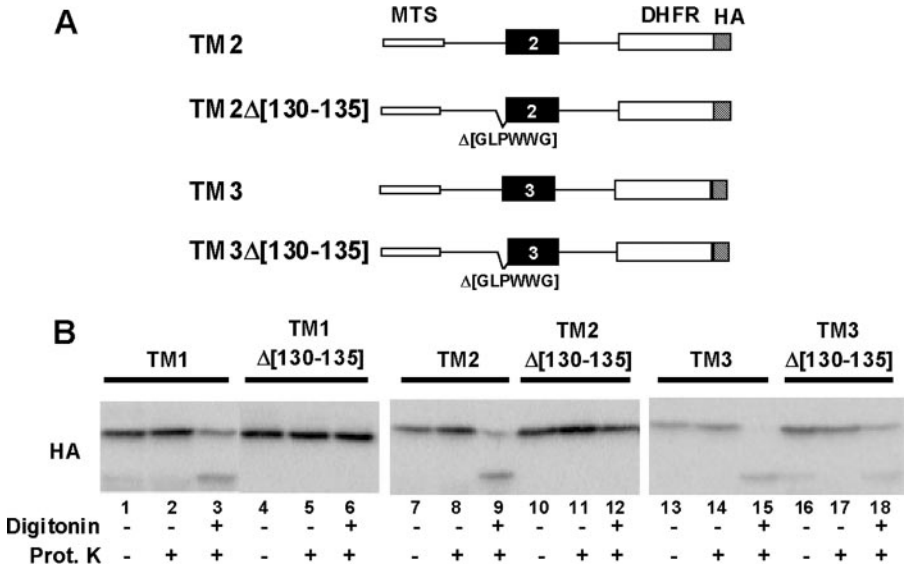

FIGURE 4. **Effect of the hexapeptide sequence on the N-terminal export of TM2 and TM3.** *A*, schematic diagram of the TM2 and TM3 constructs. *B*, protease protection analysis to detect the submitochondrial localization. Mitochondria were treated with proteinase K with or without 0.1% digitonin and analyzed as in Fig. 2*B*. *DHFR*, dihydrofolate reductase; *Prot. K*, proteinase K.

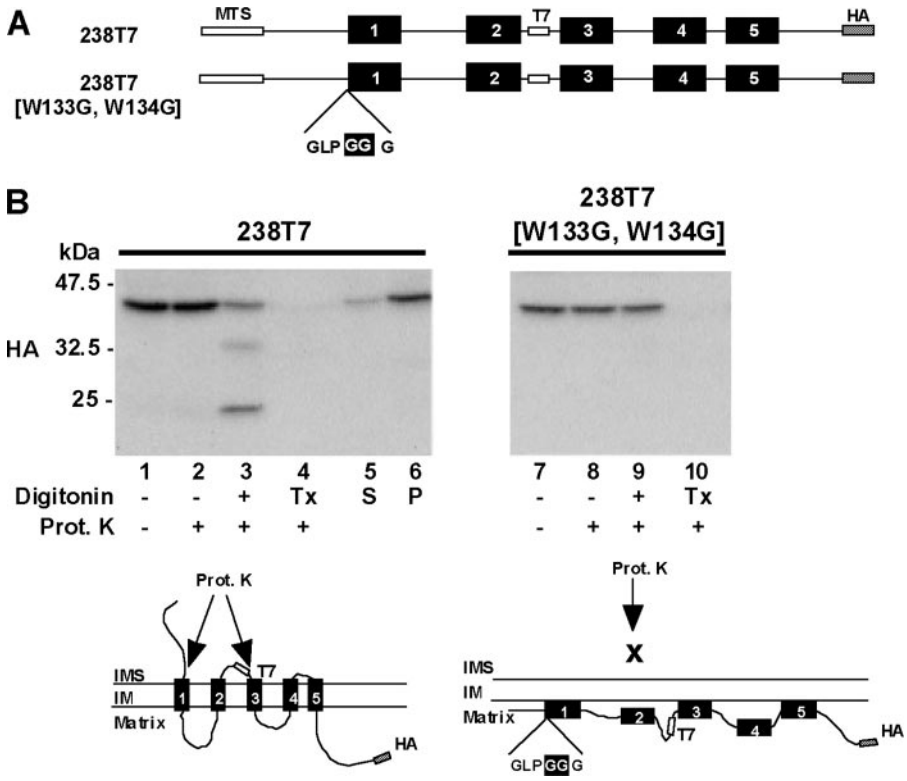

FIGURE 5. **Intermembrane segment export of the short loop between TM2 and TM3 using T7-tag insertion constructs.** *A*, schematic diagram of 238T7 and 238T7(W133G,W134G). *B*, submitochondrial localization was examined by protease treatment in the presence of 0.1% digitonin or 1% Trion X-100 (*Tx*) as described in Fig. 1*E*. *Prot. K*, proteinase K; *IM*, *inner membrane*; *S*, supernatant; *P*, membrane fraction.

The Hexapeptide Functions as a General N-terminal Export Signal in the N-terminal Vicinity of an Appropriate TM—To examine whether the hexapeptide sequence affects topogenic function of TMs other than TM1 in Oxa1, N-terminal export was investigated for constructs in which the TM1 segment (mean hydrophobicity, 2.2) in the reporter (see Fig. 2*A*) was replaced with TM2 or TM3 (mean hydrophobicity 2.1 and 1.9, respectively; Fig. 4*A*). In the original context, TM2 and TM3 assume a Nin-Cout and Nout-Cin topology in the inner membrane, respectively. When TM1 was replaced with TM2 or TM3, N-terminal export was essentially supported (Fig. 4*B*, *lanes 7–9* and *13–15*). In contrast, when the hexapeptide was deleted from the constructs, the export activity was compromised (*lanes 10–12* and *16–18*), thereby suggesting that the species-conserved hexapeptide, when appended to the N terminus near an appropriate TM, cooperates with the TM to function as the N-terminal export signal irrespective of the TM authentic orientation in the original context.

Export of Both the N-terminal and L2 Regions Depends on the Hexapeptide Sequence—The IMS loops L2 and L4 of rOxa1 were not cleaved by proteinase K under the MOM-permeabilized conditions, because only the fragment corresponding to the size of the N-terminal segment-trimmed rOxa1 was detected (see Fig. 1*D*). To examine the translocation of the loop region along with the N-terminal export, the T7 tag was introduced into the middle of L2 (238T7; Fig. 5*A*). Mitochondria harboring 238T7 produced a major 25-kDa band when treated with proteinase K under the MOM-permeabilized condition; the size of the band corresponded to the fragment containing the segment downstream from TM3, clearly indicating that the loop region was exposed to the IMS (Fig. 5*B*, *lanes 2* and *3*). The hexapeptide mutant, 238T7(W133G,W134G), however, did not produce the 25-kDa band, indicating that mutation also compromised the translocation of the loop region (Fig. 5*B*, *lanes 8* and *9*). These findings indicated that translocation of the loop region occurred concurrently with the N-terminal export, a mode that supports the deduced mechanism in which all five TMs are integrated as a block coupled with IMS export of the N-terminal segment (see Fig. 2).

Exogenously Expressed rOxa1 Precursor Is Integrated into the MIM by Endogenous Oxa1—The involvement of mammalian Oxa1 in its insertion into the MIM was analyzed using Oxa1 knockdown HeLa cells. Under optimal conditions, the level of

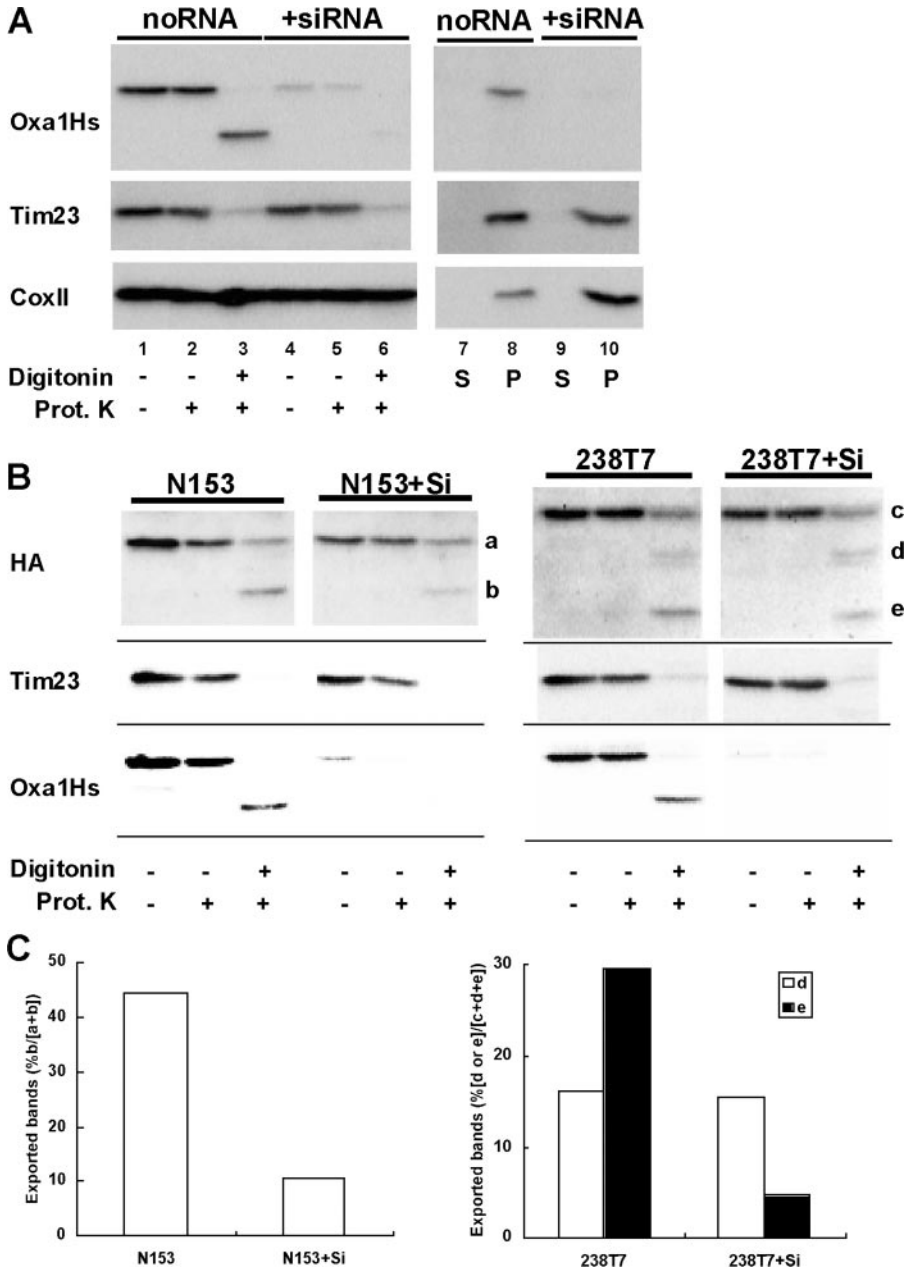

FIGURE 6. **Effect of Oxa1Hs knockdown on the N-terminal export and translocation of the hydrophilic loop between TM2 and TM3 of rOxa1.** *A*, protease protection analysis of the submitochondrial localization of Tim23 and cytochrome *c* oxidase subunit II (*CoxII*) after Oxa1Hs knockdown. Mitochondria isolated from HeLa cells transfected with (+*Si*) or without (*no RNA*) 100 nM siRNA were treated with the protease in the presence of 0.1% digitonin, as described in Fig. 1*E*. *Prot. K*, proteinase K. *B*, protease protection analysis of N153 and 238T7 transfected into the Oxa1Hs-knockdown (+*Si*) HeLa cells. The proteins in the isolated mitochondria were examined with protease treatment in the presence of 0.1% digitonin, as described in the legend for Fig. 2*B*. *a* and *c*, non-exported bands; *b*, *d*, and *e*, exported bands. *C*, effect of endogenous Oxa1 siRNA on the export of the N-terminal segment and the loop between TM2 and TM3. Export is shown as a percentage of the value of the exported band (*b* in N153/N153+Si, *d* and *e* in 238T7/238T7+Si) to the total densitometric value (*a* + *b* in N153/N153+Si, *c* + *d* + *e* in 238T7/238T7+Si).

endogenous Oxa1 (Oxa1Hs) decreased to ~20% 48 h after siRNA transfection (Fig. 6*A* and supplemental Fig. 4*A*). Immunofluorescence microscopy confirmed the knockdown of Oxa1 in HeLa cells (supplemental Fig. 4*B*). Fluorescence-activated cell sorter analysis of mitochondria that were stained with MitoTracker Red showed that the mitochondrial membrane potential was not altered by the knockdown (data not shown). In yeast, membrane insertion of cytochrome *c* oxidase subunit II shows remarkable Oxa1 dependence (13). In mammalian cells, however, the steady state level of cytochrome *c* oxidase subunit II was not affected by Oxa1 knockdown (Fig. 6*A*, *lanes 1* and *4*), and cytochrome *c* oxidase subunit II remained resistant to alkaline extraction (Fig. 6*A*, *lanes 7–10*), indicating that mitochondrial respiratory function was not compromised by Oxa1 knockdown.

We then analyzed the involvement of Oxa1 in the biogenesis of exogenously expressed rat Oxa1 constructs. N153 or 238T7 was exogenously expressed in the Oxa1-depleted HeLa cells. The IMS export of the N-terminal segment of N153 as well as co-export of the N-terminal segment and L2 of 238T7 was clearly compromised by Oxa1 knockdown (Fig. 6, *B* and *C*). These results suggested that Oxa1 mediated the N-terminal export and translocation of the loop region of the exogenously expressed rOxa1.

DISCUSSION

Membrane topogenesis of mammalian Oxa1 was investigated in HeLa cells. The N-terminal 45-amino acid residue segment constituted a cleavable mitochondrial matrix-targeting signal. Deletion of the matrix-targeting signal resulted in the remainder of the segment being transported to the ER. TMs in mature Oxa1 have relatively high hydrophobicity (the mean hydrophobicity of TM1–5 is 2.2, 2.1, 1.9, 1.4, and 1.1, respectively; see Ref. 23 for a comparison with those of ER membrane proteins) that potentially function as the ER signal-anchor sequence; they are recognized cotranslationally by the signal recognition particle and are targeted to the ER membrane as is the case for ABCme (22). The N-terminal MTS of Oxa1 precursor, thus, functions as the sequence that prevents ER translocation, probably by preventing cotranslational recognition of the TMs by the signal recognition particle.

To determine IMS export of the N-terminal segment and of mature Oxa1, the target precursor constructs were expressed in HeLa cells, and the isolated mitochondria were analyzed to determine the proteinase K susceptibility of the IMS-exported

domains after MOM permeabilization; this enabled efficient and quantitative analyses compared with the *in vitro* import approach. The pre-rOxa1-dihydrofolate reductase constructs with a serial deletion of the TM segments revealed that the MTS and all five TMs were required for complete N-terminal export and correct MIM integration.

Interestingly, IMS export of the N-terminal segment and L2 was strongly compromised by removal or mutation of the species-conserved hexapeptide sequence GLPWWG that is localized near the N terminus of TM1; within this hexapeptide, the L*X*WW sequence was critical for the activity. Most conspicuously, mutation of the two tryptophan residues completely abolished IMS export of the N-terminal segment from the matrix. Furthermore, removal of TM1 also strongly compromised the export of the N-terminal segment, thus indicating that the hexapeptide sequence functions in conjunction with TM1 as the IMS export signal across the MIM. It should be noted in this context that the hexapeptide sequence-deleted mutant and TM1-deleted mutant both accumulated in the matrix in a proteinase K-resistant state. These results indicate that hydrophobic TMs remaining in the Oxa1 molecule did not arrest import across the MIM into the matrix and suggest that the MIM assembly of rOxa1 would proceed through the intermembrane space once accumulated within the matrix. Moreover, the hexapeptide sequence also functioned as the N-terminal export signal in concert with the adjacently positioned TM2 or TM3 excised from Oxa1, indicating that the hexapeptide sequence followed by a TM functions as a general MIM insertion signal from the matrix of MIM proteins in the Nout-Cin orientation. To our knowledge, there are no precedents for such a topogenic signal for MIM proteins.

We also found that the loop (L2) between TM2 and TM3 is translocated across the MIM into the IMS concomitant with the export of the N-terminal segment of mature Oxa1, and most importantly, the translocation of the loop also depended on the conserved hexapeptide sequence. These results in conjunction with the data demonstrating the importance of all of the TMs (TM1-TM5) in efficient MIM integration of Oxa1 in the correct topology suggest that the mature Oxa1 imported into the matrix is inserted at once and not sequentially into the MIM, and this insertion seems to be primed by the hexapeptide sequence present just upstream of TM1, although this mode does not rule out a pairwise and synergistic insertion of TM2-TM3 and TM4-TM5 from the matrix as proposed in yeast Oxa1 (4). Although we did not demonstrate the membrane orientation of the short loop between TM4 and TM5, we consider from these lines of circumstantial evidence that it is also translocated into the IMS across the MIM depending on the hexapeptide sequence.

It is not known why rOxa1 mutants devoid of several TMs are inefficiently integrated into the MIM despite the fact that they are all completely imported into the matrix. Beck *et al.* (24) demonstrated that a bacterial Oxa1 homologue, YidC, is involved in the insertion of a polytopic inner membrane protein by binding concurrently to the multiple transmembrane segments during its biogenesis. Also, YidC functions in the folding of a membrane protein during its insertion (25). It is conceivable, therefore, that deletion of TMs resulted in an overall conformational change in the rOxa1 mutants, which might be trapped in the endogenous Oxa1 machinery through surface-exposed TMs, leading to inhibition of N-terminal segment export. rOxa1 with a complete set of TMs might be required for correct folding and rapid release from the Oxa1 machinery.

What is the function of the L*X*WW motif in the export of the N-terminal segment? It is possible that L*X*WW is required both for maintaining the integration-competent conformation of mature Oxa1 once localized in the matrix and for the priming of MIM integration of the whole Oxa1 molecule. In this context, Lemaire *et al.* (26) demonstrated in yeast the importance of the two tryptophans (128–129) corresponding to those present in the yeast hexapeptide sequence for the function of Oxa1; the missense mutations (WW to AA) led to a severe thermo-sensitive phenotype and specific defects of cytochrome *c* oxidase formation at high temperature caused by an impaired MIM insertion of cytochrome *c* oxidase subunit II. They identified a methyltransferase-like MIM protein, Oms1p, as a multicopy suppressor of the mutation. The components that recognize the hexapeptide sequence remain to be identified, although a data base search of the mammalian genome failed to identify a mammalian homologue of Oms1p, and biogenesis of cytochrome *c* oxidase subunit II does not depend on Oxa1 in mammals.

Knockdown of mammalian Oxa1 by siRNA resulted in defective export of the N-terminal segment and L2 of exogenously expressed Oxa1, suggesting that MIM integration of Oxa1 is mediated by Oxa1 itself and that mutations in the hexapeptide sequence might affect Oxa1 function through defective membrane topogenesis. The cellular function of mammalian Oxa1, however, remains to be analyzed, because cytochrome *c* oxidase subunit II (Cox2) biosynthesis, the membrane potential across the MIM, and mitochondrial morphology were neither affected by knockdown of mammalian Oxa1, although Oxa1 deficiency in yeast leads to defects in the biosynthesis of all of the respiratory complexes.

Acknowledgments—We thank Toshihiko Oka and members of the Mihara laboratory for productive discussions.

REFERENCES

1. Herrmann, J. M., and Neupert, W. (2003) *IUBMB Life* **55,** 219–225
2. Rehling, P., Brandner, K., and Pfanner, N. (2004) *Nat. Rev. Mol. Cell Biol.* **5,** 519–530
3. Herrmann, J. M., Koll, H., Cook, R. A., Neupert, W., and Stuart, R. A. (1995) *J. Biol. Chem.* **270,** 27079–27086
4. Herrmann, J. M., Neupert, W., and Stuart, R. A. (1997) *EMBO J.* **16,** 2217–2226
5. Rojo, E. E., Guiard, B., Neupert, W., and Stuart, R. A. (1999) *J. Biol. Chem.* **274,** 19617–19622
6. Jia, L., Dienhart, M., Schramp, M., McCauley, M., Hell, K., and Stuart, R. A. (2003) *EMBO J.* **22,** 6438–6447
7. Szyrach, G., Ott, M., Bonnefoy, N., Neupert, W., and Herrmann, J. M. (2003) *EMBO J.* **22,** 6448–6457
8. Ott, M., Prestele, M., Bauerschmitt, H., Funes, S., Bonnefoy, N., and Herrmann, J. M. (2006) *EMBO J.* **25,** 1603–1610
9. Bonnefoy, N., Chalvet, F., Hamel, P., Slonimski, P. P., and Dujardin, G. (1994) *J. Mol. Biol.* **239,** 201–212
10. He, S., and Fox, T. D. (1997) *Mol. Biol. Cell* **8,** 1449–1460
11. Hell, K., Herrmann, J., Pratje, E., Neupert, W., and Stuart, R. A. (1997)

FEBS Lett. **418,** 367–370
12. Hell, K., Herrmann, J. M., Pratje, E., Neupert, W., and Stuart, R. A. (1998) *Proc. Natl. Acad. Sci. U. S. A.* **95,** 2250–2255
13. Hell, K., Neupert, W., and Stuart, R. A. (2001) *EMBO J.* **20,** 1281–1288
14. Stuart, R. (2002) *Biochim. Biophys. Acta* **1592,** 79–87
15. Samuelson, J. C., Chen, M., Jiang, F., Möller, I., Wiedmann, M., Kuhn, A., Phillips, G. J., and Dalbey, R. E. (2000) *Nature* **406,** 637–641
16. Serek, J., Bauer-Manz, G., Struhalla, G., van den Berg, L., Kiefer, D., Dalbey, R., and Kuhn, A. (2004) *EMBO J.* **23,** 294–301
17. Reif, S., Randelj, O., Domanska, G., Dian, E. A., Krimmer, T., Motz, C., and Rassow, J. (2005) *J. Mol. Biol.* **354,** 520–528
18. Herrmann, J. M., and Bonnefoy, N. (2004) *J. Biol. Chem.* **279,** 2507–2512
19. Jia, L., Dienhart, M. K., and Stuart, R. A. (2007) *Mol. Biol. Cell* **18,** 1897–1908
20. Ishihara, N., and Mihara, K. (1998) *J. Biochem.* **123,** 722–732
21. Vestweber, D., and Schatz, G. (1988) *EMBO J.* **7,** 1147–1151
22. Miyazaki E., Kida Y., Mihara K., and Sakaguchi M. (2005) *Mol. Biol. Cell* **16,** 1788–1799
23. Kanaji, S., Iwahashi, J., Kida, Y., Sakaguchi, M., and Mihara, K. (2000) *J. Cell Biol.* **151,** 277–288
24. Beck, K., Eisner, G., Trescher, D., Dalbey, R. E., Brunner, J., and Müller, M. (2001) *EMBO Rep.* **2,** 709–714
25. Nagamori, S., Smirnova, I. N., and Kaback H. R. (2004) *J. Cell Biol.* **165,** 53–62
26. Lemaire, C., Guibet-Grandmougin, F., Angles, D., Dujardin, G., and Bonnefoy, N. (2004) *J. Biol. Chem.* **279,** 47464–47472